Photocurrent Induced by Nonradiative Energy Transfer from Nanocrystal Quantum Dots to Adjacent Silicon Nanowire Conducting Channels: Toward a New Solar Cell Paradigm

ARTICLE *in* NANO LETTERS · OCTOBER 2009

Impact Factor: 13.59 · DOI: 10.1021/nl903104k · Source: PubMed

NANO LETTERS

XXXX
Vol. xx, No. x
-

Photocurrent Induced by Nonradiative Energy Transfer from Nanocrystal Quantum Dots to Adjacent Silicon Nanowire Conducting Channels: Toward a New Solar Cell Paradigm

Siyuan Lu,[†] Zachary Lingley,[‡] Tetsuya Asano,[‡] Daniel Harris,[‡] Tymon Barwicz,[§] Supratik Guha,[§] and Anupam Madhukar*[,†,‡]

Department of Physics, Mork Family Department of Chemical Engineering and Materials Science, University of Southern California, Los Angeles, California 90089, and IBM J. T. Watson Research Center, Yorktown Heights, New York 10598

Received September 19, 2009; Revised Manuscript Received October 14, 2009

ABSTRACT

We report the observation of photocurrent in silicon nanowires induced by nonradiative resonant energy transfer (NRET) from adjacent layers of lead sulfide nanocrystal quantum dots using time-resolved photocurrent measurements. This demonstration supports the feasibility of a new solar cell paradigm (Lu, S.; Madhukar, A. *Nano Lett.* 2007, *7*, 3443−3451) that exploits NRET between efficient photon absorbers and adjacent nanowire/quantum well high-mobility charge transport channels and could offer a viable alternative to the limitations of carrier transport and collection faced by excitonic solar cells.

Conversion of solar energy to power in a material system involves the following four fundamental physical steps: (1) the absorption of solar photons and the creation of excitons; (2) separation of the exciton into individual electron and hole pair; (3) transport of the electron and hole to their respective collection electrodes; and (4) collection of the electron and hole at the electrodes. The overall efficiency of the solar cell thus depends upon the product of the efficiency of each of these steps. It is well-known that the in conducting polymer based excitonic solar cells (organic/quantum dot hybrid or all-organic),[2,3] the absorption of photon is nearly 100% efficient. The bottleneck to high conversion efficiencies beyond the current state of the art of ∼6% is the low value of the product of efficiencies of exciton separation and carrier transport in the organic media. The low efficiency of these two steps is tied, respectively, to the limitation of organic electronic materials, namely their large exciton binding energy (few hundreds of meV) and low carrier mobility (∼ 1 $cm^2/V{\cdot}sec$).

Recently, we proposed[3] a photovoltaic solar energy conversion paradigm based on nonradiative energy transfer (NRET) from nanocrystal quantum dots (QDs) to adjacent high mobility inorganic conducting channels as schematically shown in Figure 1a from ref 3. We demonstrated[3] the feasibility of such NRET through extraction of the energy transfer rate from measurements of the time-resolved photoluminescence decay of the PbS quantum dots adjacent to an GaAs/InGaAs/GaAs quantum well as the acceptor channel. In this letter, we take this concept one step further by reporting measurement of photocurrent in silicon nanowires arising from NRET from adsorbed PbS QDs. We choose silicon nanowires for its universal appeal and mature technology, anticipating the development of efficient NRET-based solar cells in a cost-effective manner. Silicon being the most widely employed and advanced semiconductor technology, we are of the view that creation of NRET solar cells within the silicon material system based technology platform will leverage from the vast infrastructure already in place. We note that our proposed NRET-based solar cell paradigm offers the following advantageous features: (1) high absorption efficiency of the QDs, (2) upon absorption, resonant exciton transfer to the adjacent inorganic energy acceptor channel accompanied by spontaneous exciton break-up into unbound electron and hole owing to the typical very low (10 meV) exciton binding energy in the inorganic channel, and (3) efficient electron and hole transport in the

* To whom correspondence should be addressed. E-mail: madhukar@usc.edu. Phone: 1-213-740-4323. Fax: 1-213-740-4333.
[†] Department of Physics, University of Southern California.
[‡] Mork Family Department of Chemical Engineering and Materials Science, University of Southern California.
[§] IBM J. T. Watson Research Center.

10.1021/nl903104k CCC: $40.75

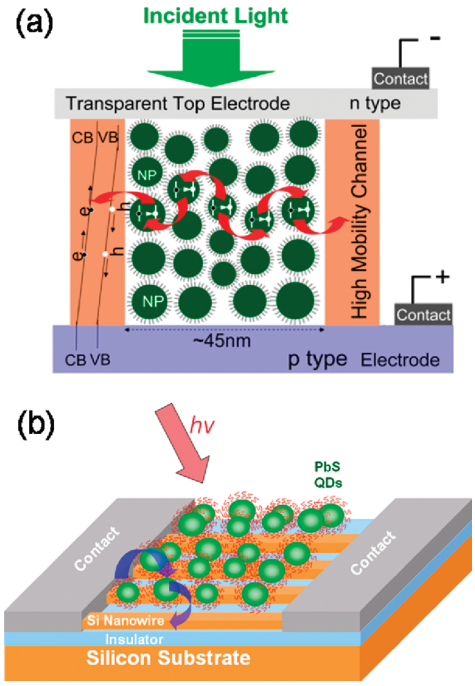

Figure 1. (a) Schematic of NRET-based all-inorganic solar cell architecture. (b) Schematic showing a structure comprising QDs deposited on horizontal Si nanowire high-mobility conducting channels serving as the proof-of-concept measurement platform for our proposed NRET based solar cells.

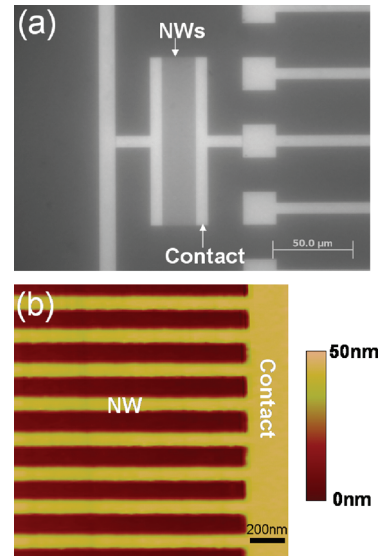

Figure 2. (a) A light microscope image showing a horizontal Si nanowire array device used for the photocurrent measurements. (b) An AFM image showing individual Si nanowires in the array.

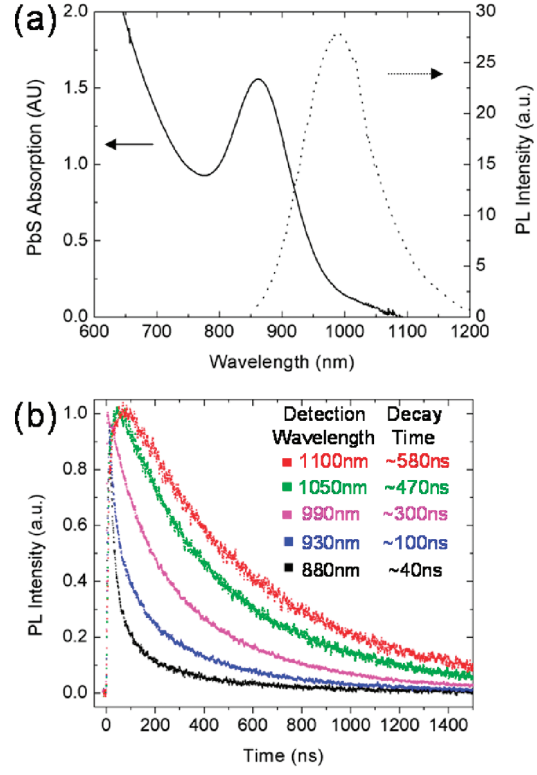

Figure 3. (a) Absorption spectrum of PbS nanocrystal quantum dots in toluene solution (solid line) and photoluminescence spectrum of PbS nanocrystals deposited on silicon nanowire arrays (dotted line). The PL excitation wavelength is 850 nm. (b) Time-resolved PL spectra of the QDs on the nanowire array. Detection wavelength: 1100 nm (red), 1050 nm (green), 990 nm (magenta), 930 nm (blue), 880 nm (black). Excitation at 800 nm. Pulse energy density 0.25 mJ/cm^2. Excitation condition is the same as that employed for photocurrent measurement.

inorganic channels owing to their high mobility (~100−1000 cm^2/V•sec). Hence, as argued in ref 3, the all inorganic QD-adjacent high mobility charge transport channel architecture has the potential of circumventing the bottlenecks of charge carrier generation and/or transport faced by the polymeric excitonic solar cells.

To demonstrate the photocurrent in the silicon nanowire transport channels arising from NRET, a planar nanowire array sample geometry, as depicted in Figure 1b, is utilized. The silicon nanowire arrays are fabricated using e-beam lithography starting from a p-type (100) silicon on insulator (SOI) wafer of resistivity 10 Ω•cm. The nanowires dimensions are 40 ± 10 nm wide, 30 nm high, 20 μm long along the [011] direction. A nanowire device consists of 500 nanowires of pitch 200 nm. Illustrative optical microscope image and atomic force microscope (AFM) image of the horizontal silicon nanowire array device is shown in Figure 2. The Si nanowires are connected through ion-implanted p^+ silicon (~0.002 Ω•cm) to metal contact pads. The procedure for Si nanowire sample fabrication and the electrical characterization of the nanowires is detailed in Supporting Information S1. The PbS QDs are synthesized using a method modified from Hines et al.[4] as detailed in Supporting Information S2. The as-synthesized QDs have PbS core average diameter of ~2.5 nm and are covered by oleic acid ligands. The absorption spectrum of the PbS QDs in toluene solution is shown in Figure 3a (solid line). The quantum yield of the as-synthesized QDs in toluene solution is measured to be ~40%.[5] A multilayered PbS QD thin-film of thickness ~200 nm (measured by AFM) was formed by dry-cast 2 mg/mL QD solution onto the nanowire array at room temperature. The time-integrated PL spectrum of the QDs on the nanowire array is shown in Figure 3a (dotted line). The peak of the QD emission is at 990 nm with a fwhm of ~130 nm. Note that the PL emission is dominated by the

quantum dots in the body of the film, away from the region adjacent to the Si nanowires. The time-resolved PL spectra of the QDs on the nanowire array as a function of detection wavelength (equivalently quantum dot size) are shown in Figure 3b. These are measured under the same excitation condition as used for photocurrent measurements reported in the following. Although the decay behavior, as discussed in ref 3, can be more complex than a single exponential decay, owing to inter-QD energy transfer, to a first order, fitting the decay with a single exponential provides a reasonable estimate of the range of decay time scales as a function of the emission wavelength, that is, the quantum dot size. Note that this decay time is the inverse of the sum of all rates representing possible decay channels.[3] Such a fitting gives the range of decay times from ~100 ns for 930 nm emission from the small QDs to ~300 ns for 990 nm emission (PL peak), and ~470 ns for 1050 nm emission from the large QDs. Note also in Figure 3b the initial rise in the PL intensity for the longest wavelength emissions, an indication of the inter-QD NRET from the smaller to the larger dots as reported in ref 3. Indeed, such transfer makes the decay time for smaller QDs shorter than it would be in the absence of the larger dots as neighbors.

To unambiguously measure the NRET-induced photocurrent, it is best to perform a time-resolved measurement in which light pulse-induced photocurrent in the Si nanowires with the QDs dispersed on top is compared to the photocurrent in Si nanowires without any QDs on top. The electron−hole pairs generated in the silicon nanowires due to direct photon absorption in the nanowires will be swept away extremely rapidly by a modest electric field across the wires. By contrast, the NRET time being several hundred nanoseconds,[3] its contribution to the photocurrent will occur on a similarly longer time scale, thus separating the contribution to the total measured photocurrent into its two components, those electrons and holes generated owing to NRET and those generated due to direct absorption in nanowires. Comparing the relative weight of these two components, the enhancement of photocurrent due to NRET and the NRET efficiency can be assessed, eliminating uncertainties arising from common artifacts, especially those caused by optical alignment and variation in incident light power density.

For the time-resolved photocurrent measurements, the incident angle of the excitation is ~45°. Pulse excitation energy density is estimated to be ~0.25 mJ/cm^2. An electrical field of 4.5 × 10^3 V/cm was applied to the nanowires. The expected time-of-flight for the carriers to be swept out of the 20 μm long nanowire under such an electric field is ~4 ns (we conservatively estimate the carrier mobility to be ~100 cm^2/sec•V). The photocurrent generated in the nanowire arrays with and without QDs is directly amplified and measured using a combination of box-car averaging and lock-in technique. All measurements are performed at room temperature. To minimize the photobleaching of QDs and to ensure the repeatability of experiments, the measurements were performed with the samples placed in a cryostat pumped to ~1 × 10^{-6} torr. The details of the time-resolved photocurrent measurements and the instrumentation are

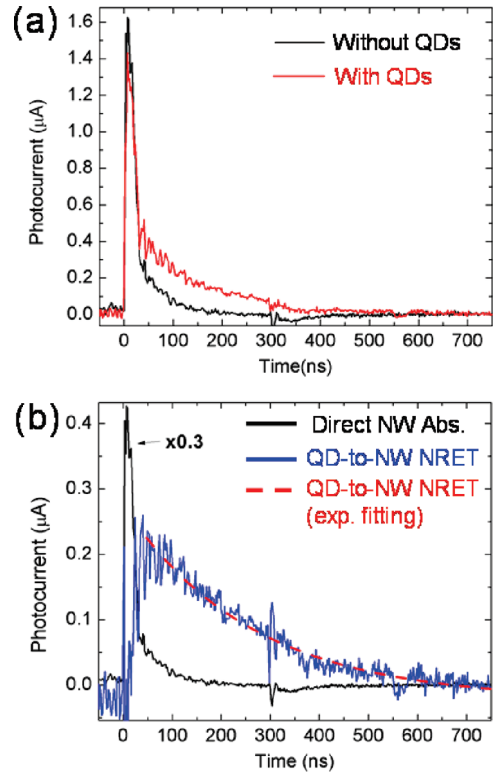

Figure 4. (a) Time-resolved photocurrent measured in the Si nanowire conducting channels with (red curve) and without (black curve) QDs deposited. (b) Photocurrent in Si nanowires contributed from direct nanowire absorption (black curve) and from QD-to-nanowire NRET (blue curve). The red dashed curve is the single exponential fitting of the QD-to-nanowire NRET contributed photocurrent. The fitted exponential decay time constant is ~260 ns.

presented in Supporting Information S3. Finally, we note that as the samples, as noted in the preceding, are prepared by dry-casting QDs from the solution onto the silicon nanowires with contacts in place, the QD film unavoidably covers some part of the contact regions as well. To avoid any confusion about any contribution to the measured photocurrent coming from the quantum dot film, we performed measurements on control samples in which QD film was deposited on structures comprising metal contacts of the same separation (as in the nanowire sample) on glass substrate. Indeed, no measurable photocurrent was detected. The lack of photoconductivity in the QD film is not surprising since the QDs are well protected by oleic acid ligands and the applied electric field is fairly moderate (4.5 × 10^3 V/cm).

In Figure 4a, we show the photocurrent response measured for nanowire samples without (black) and with (red) QDs dispersed on top of the Si nanowires for excitation at 800 nm. The photocurrent without QDs shows a peak of fwhm ~22 ns immediately after the light pulse and is due to the direct photon absorption and exciton creation in the nanowires. As noted above, the expected time-of-flight for the carriers to be swept out of the nanowires is ~4 ns. The observed width of the photocurrent peak is a result of the convolution of the actual photocurrent signal with the instrumental response function (IRF)[6] of the measurement electronics but this does not affect the magnitude of the time

integrated photocurrent signal underneath the photocurrent peak. The integrated photocurrent for the sample with the quantum dots is 1.79 times that for the bare silicon nanowires, indicating a significant contribution arising from the presence of the QDs. The photocurrent response in nanowires with QDs (Figure 4a, red curve) shows two features. First, the immediate peak after the light pulse which corresponds to the direct absorption in the nanowires is reduced to ~90% compared to that observed without QDs. This reduction is consistent with the estimated ~10% absorption of the 800 nm excitation light through the ~200 nm thick QD layer.[7] Second, a significantly enhanced tail of photocurrent spanning ~500 ns after the excitation pulse, indicating a contribution from energy transfer from QDs to nanowires. Note that the nanowire absorption of the photons generated by the radiative decay of QDs (being at longer wavelengths) is less efficient than the absorption of exciting photons at 800 nm. Thus the enhanced tail cannot have a major contribution from radiative energy transfer (i.e., QDs emitting and nanowires absorbing) and is predominantly due to the nonradiative resonant energy transfer (NRET) from the QDs to the nanowires.

A quantitative measure of the QD-to-nanowire NRET contributed photocurrent component and the NRET efficiency can thus be obtained as follows. The photocurrent in the nanowires with QDs, $I_{NW+QD}(t)$, (Figure 4a, red curve) can be decomposed into two components

$$\begin{aligned} I_{NW+QD}(t) &= I_{NW}(t) + I_{NRET}(t) \\ &= T{\cdot}I'_{NW}(t) + I_{NRET}(t) \end{aligned} \quad (1)$$

where $I_{NW}(t)$ represents the photocurrent component generated in the QD deposited nanowires owing to the direct light absorption in the nanowires and $I_{NRET}(t)$ is the photocurrent component induced by the QD-to-nanowire NRET. It is reasonable to expect that $I_{NW}(t) = T{\cdot}I'_{NW}(t)$ where $I'_{NW}(t)$ is the photocurrent measured in the nanowires without QD deposition (Figure 4a, black curve) and T is the transmission of the excitation light through the QD layer.

By taking the ratio of the two measured photocurrent peak values in Figure 4a corresponding to light incident on nanowires with and without the adsorbed QDs, we find that the operative transmission through the QD layer (T) is 88%. Using this value of T and the measured $I_{NW+QD}(t)$and $I'_{NW}(t)$ from eq 1, we obtain $I_{NW}(t)$ (the nanowire direct absorption contributed photocurrent) and $I_{NRET}(t)$ (the QD to Si nanowire NRET contributed photocurrent). These are plotted in Figure 4b in black and blue, respectively. A fitted exponential decay to the $I_{NRET}(t)$ in Figure 4b gives a decay constant of ~260 ns. Recall that owing to the rapid inter-QD NRET, the NRET to the adjacent acceptor channels is dominated by the larger QDs nearest to the accepting channels,[3] here the Si nanowires. When compared to the PL decay time constants of these larger dots that are seen in Figure 3b to be longer than ~300 ns, the wavelength integrated photocurrent current decay time being shorter is consistent with the expected presence of NRET to the adjacent nanowire channels.

Using the same procedure as described above, we determined the photocurrent contributions from direct nanowire absorption ($I_{NW}(t)$) and NRET from QDs to nanowires ($I_{NRET}(t)$) as a function of the excitation wavelength in the range 775−900 nm. These time-integrated spectrally resolved values are plotted in Figure 5. Note that the relative contribution of the NRET-induced photocurrent ($I_{NRET}(t)$, triangles in Figure 5) can be as large as ~3 times the photocurrent contributed by direct nanowire absorption ($I_{NW}(t)$, squares in Figure 5) at 875 nm excitation near the peak of the QDs absorption spectrum (solid line in Figure 5). As expected, the time-integrated photocurrent due to direct nanowire absorption ($I_{NW}(t)$, squares in Figure 5) as a function of wavelength, matches the extinction coefficient of Si (dotted line in Figure 5) which represents the light absorption in the silicon nanowires. More importantly, the time-integrated photocurrent attributable to QDs-to-nanowires NRET ($I_{NRET}(t)$, triangles in Figure 5) follows reasonably the absorption spectrum of the QDs in solution (solid line in Figure 5). The resemblance between time-integrated $I_{NRET}(t)$ and the QD absorption spectrum indicates that the efficiency of NRET from QDs to nanowires is relatively insensitive to the excitation wavelength. This is not surprising since following the photoexcitation of the QDs, the excitons relax to their ground states on a subpicosecond to picosecond time scale,[8] much faster than NRET. Thus, independent of the excitation wavelength, the initial state involved in the QD-to-nanowire NRET is the ground state excitons in the individual QDs, leading to the transfer efficiency being insensitive to the excitation wavelength. Thus while the NRET induced photocurrent in the acceptor channels and the QD PL both have exponential decay, the former is faster than the latter for the QDs of the larger sizes that are the dominant gatekeepers of energy transfer.

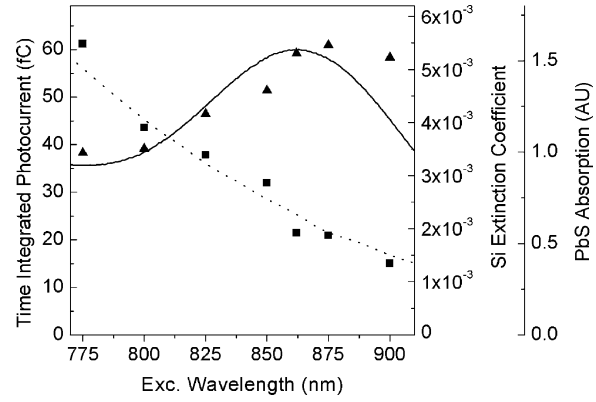

Figure 5. The time-integrated photocurrent attributed to direct absorption in silicon nanowires, $I_{NW}(t)$ (squares), and to NRET from PbS QDs to the nanowires, $I_{NRET}(t)$ (triangles), as a function of excitation wavelength. Dotted line shows the Si extinction coefficient representing the light absorption in the silicon nanowires. Solid line shows the absorption spectrum of PbS QDs in toluene. The plotted PbS absorption is normalized to its values at 800 nm.

To semiquantitatively estimate the efficiency of NRET, defined as the number of e-h pairs created in the nanowires due to NRET divided by the number of excitons created in the QDs immediately adjacent to the nanowires, we consider, without loss of generality, excitation at 800 nm. The

absorption cross-section of a monolayer of QDs surrounding the silicon nanowire (on the top and on the two sidewalls) is ~1800 nm^2 (ref 9). We recall that the NRET rate (R_{NRET}) is related to the intradot radiative decay rate (R_{Rad}) through the expression $R_{NRET} = (R_0/r)^n R_{Rad}$ in which r is the separation between the two dipoles, R_0 is the so-called Förster radius, which depends upon the strengths of the two dipoles involved and other material and geometric factors, and n is an integer varying from 6 to 3 for transfer from a three-dimensionally (3D) confined state to 3D, 2D, 1D, and 0D confined states, respectively.[10] As we previously reported,[3] the particular QDs employed here have a nearest-neighbor inter-QD transfer efficiency of ~80% and thus only the excitons created in the second through fifth monolayer of QDs next to a nanowire can be transferred with some efficiency (>40%) to the QD layer in immediate contact with the nanowires (from which the QD-to-nanowire NRET can occur efficiently).[3] Thus, the QD excitation region for QDs-to-nanowire NRET we estimate has an effective absorption cross-section ~3600−9000 nm^2. The absorption cross-section of a silicon nanowire is ~1500 nm^2 (ref 11). Consequently, the number of excitons generated in the QD layer (n_{ex-QD}) versus in the nanowire (n_{ex-NW}) is a ratio that ranges over ~2.4 to 6 ($n_{ex-QD}/n_{ex-NW} \sim 2.4-6$). Moreover, the ratio of the number of excitons transferred from QDs to nanowires (n_{NRET}) to the number of excitons generated in the NW (n_{ex-NW}), we presume is equal to the ratio of the NRET contributed photocurrent to direct nanowire absorption contributed photocurrent (time integrated, see Figure 5) which is measured to be ~0.9 (thus $n_{NRET}/n_{ex-NW} \sim 0.9$). We thus estimate the NRET efficiency, $\eta_{NRET} = n_{NRET}/n_{ex-QD} = [n_{NRET}/n_{ex-NW}]/[n_{ex-QD}/n_{ex-NW}]$, to be in the range of ~15−38%. Note that the rate of NRET from QDs (3D confined states) to silicon nanowires of ~30 nm in diameter involving bulk states (i.e., no quantum confinement) is expected to follow a $1/r^3$ dependence where r is the distance from the center of QDs to the surface of the nanowires. The use of narrower structures (quantum wells and quantum wires) involving quantum confined states will enhance the NRET transfer rate for the same separation r given all other features the same as has been noted before.[3,10,12,13]

In conclusion, we have provided evidence of photocurrent in silicon nanowire charge transport channels induced by nonradiative resonant energy transfer (NRET) from QDs in close contact using time-resolved photocurrent measurements at room temperature. For the unoptimized combination of PbS nanocrystal quantum dots dispersed upon silicon nanowires employed here for demonstration purposes, the photocurrent due to NRET can be as large as 3 times the photocurrent due to direct light absorption in the Si nanowires for excitation near the absorption peak of the QDs and the NRET efficiency is calculated to lie between ~15−38%. We expect that the NRET efficiency in the present results can be further improved by reducing the distance between QDs and nanowires through, for example, reducing the length of QD ligands and reduction in nanowire dimensions to induce quantum confinement. This demonstration of efficient NRET induced photocurrent further supports the feasibility of our proposition[3] of a new solar energy conversion paradigm exploiting nonradiative energy transfer from efficient photoabsorbers to high mobility transport channels. Finally, though for demonstration purposes we have employed the horizontal wire array configuration owing to its easier fabrication at this stage, the vertical array geometry of Figure 1a as we originally proposed[3] is the effective architecture as it (i) allows light absorption along the wire length, thus shortening the lengths to only of order a few micrometers sufficient for near 100% light absorption in the quantum dots and (ii) allows shorter nanowire pitch for higher and optimal realization of light absorption versus energy transfer and charge transport volume fill factor.

Acknowledgment. This work is supported by AFOSR Grant FA9550-08-1-0146 (Program Manager Dr. Kitt Reinhardt). The authors gratefully acknowledge the efforts of the staff of the Microelectronics Research Laboratory (MRL) at the IBM T. J. Watson Research Center where the nanowire array samples were fabricated.

Supporting Information Available: Experimental details on (1) the fabrication and characterization of the silicon nanowire samples, (2) the synthesis of the PbS nanocrystals, and (3) the instrumentation for time-resolved photocurrent measurements. This material is available free of charge via the Internet at http://pubs.acs.org.

References

(1) Huynh, W. U.; Dittmer, J. J.; Alivisatos, A. P. *Science* **2002**, *295*, 2425–2427.
(2) Kim, J. Y.; Lee, K.; Coates, N. E.; Moses, D.; Nguyen, T. Q.; Dante, M.; Heeger, A. J. *Science* **2007**, *317*, 222–225.
(3) Lu, S.; Madhukar, A. *Nano Lett.* **2007**, *7*, 3443–3451.
(4) Hines, M. A.; Scholes, G. D. *Adv. Mater.* **2003**, *15*, 1844–1849.
(5) The quantum yield of the QDs was measured by comparison to IR125 dye of known quantum yield ~11−13% at 700 nm excitation.
(6) The main contribution to the width of the IRF, we suspect, is due to the high frequency impedance of the thin lead wires connecting the contact pads to the chip holder and the coaxial cable.
(7) Molar extinction coefficient of PbS QDs at 800nm ~3×10^4 cm^{-1} M^{-1} (or QD absorption cross-section ~1.1×10^{-2} nm^2), volume density ~3×10^{19} cm^{-3}, PbS QD layer thickness ~200 nm, angle of incident for 800 nm excitation laser light ~45°.
(8) Klimov, V. I. *J. Phys. Chem. B* **2000**, *104*, 6112–6123.
(9) Molar extinction coefficient of PbS QDs at 800 nm ~3×10^4 cm^{-1} M^{-1} (or QD absorption cross-section ~1.1×10^{-2} nm^2) areal density ~7.9×10^{12} cm^{-2}.
(10) Stavola, M.; Dexter, D.; Knox, R. *Phys. Rev. B* **1985**, *31*, 2277–2289.
(11) Silicon nanowire absorption is calculated using bulk silicon dielectric function taken from *Properties of Crystalline Silicon*, (emis Datareview series, No. 20); Hull, R. , Ed.; INSPEC: London, 1999.
(12) Chanyawadee, S.; Harley, R. T.; Henini, M.; Talapin, D. V.; Lagoudakis, P. G. *Phys. Rev. Lett.* **2009**, *102*, 077402.
(13) Hernandez-Martinez, P. L.; Govorov, A. *Phys. Rev. B.* **2008**, *78*, 035314.

NL903104K